COBEM 2021 26th International Congress of Mechanical Engineering
November 22-26, 2021, Virtual Congress, Brazil

COB-2021-2284
IMPACT OF AORTIC VALVE TOPOLOGY IN THE HEMODYNAMIC FLOW PATTERNS IN THE ASCENDING AORTA

Enrico Luigi M. Perocco
Rodrigo Meyer L. Gelio
Ivan Fernney Ibanez Aguilar
Bruno Alvares de Azevedo
Angela O. Nieckele
Pontifícia Universidade Católica do Rio de Janeiro, Dept. Mechanical Eng., 22451-900, Rio de Janeiro, RJ, Brazil
enrico.perocco@aluno.puc-rio.br, rgelio@aluno.puc-rio.br, azevedo@puc-rio.br, iibanez@puc-rio.br, nieckele@puc-rio.br

Abstract. *The use of Computational Fluid Dynamics (CFD) analysis in bioengineering is increasing very rapidly since this approach provides useful information that is difficult to obtain clinically. Aiming to assist medical doctors to diagnose diseases and engineers to project equipment related to the human heart, several works can be found in the literature studying the blood flow in the human aorta. Due to the complexity of the geometry and flow, many of these works employ a simplified model of the human aorta and do not consider a realistic model of the aortic valve. In this work, the impact of the aortic valve geometry in the blood flow behavior inside a specific patient's aorta was performed by comparing it with the simple representation of the aorta valve as an orifice. For such analysis, a realistic 3D model of the human aorta was generated through the segmentation process based on a three-dimensional computed angiotomography exam of the patient. A 3D model of the aortic valve was developed based on dimensions found in the specialized literature. At the systole peak, the flow rate is high, and combined with the large diameter of the vessel, the flow behaves as turbulent. Thus, the RANS methodology was employed to obtain the flow field, where the turbulent viscosity was determined with the two-equation κ-ω SST turbulence model. The flow was numerically determined with the commercial software ANSYS Fluent. Through the analysis of hemodynamics variables such as pressure, velocity, and turbulent quantities, coherent structures were identified in the ascending aorta. It was also possible to determine regions with higher stress in the aortic wall, which is an important task since high-stress values can be related to diseases such as aortic aneurism. The present analysis showed that a simple model can provide similar main flow structures as well as stress distributions in the ascending wall as the most realistic representation of the aortic valve geometry.*

Keywords: *aortic valve, aorta, CFD, hemodynamics*

1. INTRODUCTION

Every year, cardiovascular diseases are among one of the most fatal causes of death in humans. The most widespread pathologies regarding this subject occur in the human aorta, coronary arteries and in the heart valves, and are strongly dependent of the cardiac cycle, formed by the systole and diastole. During the systole (contraction of the heart), blood flows from the left ventricle of the heart to the aorta through the opening of the aortic valve. In contrast, during the diastole (heart relaxation) the aortic valve closes, preventing blood to return to the left ventricle. Recently, Celis *et al*. (2020), Ibanez *et al.* (2020) and Johnson *et al.* (2020) have stated that heart valves have an important role in controlling the direction of the blood flow inside the aortic artery during the cardiac cycle, what can be related to the appearance of some pathologies like aneurism.

The aortic valve, located in the aortic root has a complex three-dimensional (3D) structure formed by three leaflets (TAV). These are connected at their bases to a tubular ring which provides support to the valve, approximating it geometrically to a circumferential shape (Piazza *et al.*, 2008, Haj-Ali *et al.* 2012). The aortic valve anatomy is studied and discussed specifically by Katsi *et al.* (2020), while Sahasakul *et al.* (1988) and Haj-Ali *et al.* (2012) describe the aortic valve geometry and some common geometric measures for humans' valve. As in the aorta, there are pathologies that can affect this valve, the most common being the deformity of the valve itself. As mentioned, the aortic valve has three leaflets, but in about 1 – 2% of the world population, predominantly in the male population, the aortic valve may have only two leaflets (BAV) (Yuan and Jing, 2010).

Leyh *et al.* (1999) conducted a study of the opening and closing characteristics of the aortic valve during systole. Fries *et al.* (2006) analyzed the aortic valve movement during the *in vitro* cardiac cycle after reimplantation and remodeling. Porcine aortic valve, which have a very similar behavior to humans, were used to measure opening and closing times, valve opening diameter and valve opening and closing velocities. Becsek *et al.* (2020) investigated blood flow in patients who received prosthetic heart valves. A detailed characterization of turbulent flow after the valves was performed using

computer simulations, and the results were validated against experimental measurements.

Although hearth valves have a complex shape, many researchers have studied the flow inside the aorta, representing the valve as a circular orifice. All the following references applied this approximation.

Tang *et al.* (2012) evaluated the stress field in an aorta with dissection in the aortic arch. They have outlined the relevance that low stress values may have in the atherosclerosis development. Simão *et al.* (2017) discussed the relationship between vortex formation, low levels of WSS and its interaction with the atherosclerosis process and aortic wall remodeling, aiming to identify hemodynamic patterns in aneurysmal aortas.

Gomes *et al.* (2017) performed in vitro experiments to evaluate changes in velocity, shear rate, and vorticity fields, in a model based on a patient with aortic stenosis who underwent valve implantation surgery. Different angles of valve prosthesis inclination with respect to the aortic annulus were evaluated. Celis *et al.* (2020) studied numerically the impact of prosthetic valve orifice positioning on the blood flow. Different turbulence models were tested and compared with the experimental measurements from Gomes *et al.* (2017) and the κ-ω SST model was recommended. It has been shown that small variations in slope angles can modify flow patterns.

Almeida *et al.* (2021) performed simulations in aortas of nine patients with aortic aneurysms, using the κ-ω SST turbulence model, and discussed that the angle between the direction of the blood jet entering the ascending aorta and the brachiocephalic trunk can induce flow recirculation in the posterior area, increasing pressure level at the aortic wall, what might lead to aneurysm growth.

Ibanez *et al.* (2020) carried out a numerical study, throughout the cardiac cycle, investigating the coaxial positioning of an aortic valve prosthesis, considering a patient's aorta model. The κ-ω SST turbulence model was used, and FSI (Fluid Structure Interaction) simulations were performed. Based on the results, it was suggested that an optimal position for the valve prosthesis is when it faces the aortic left wall with an inclination of 4°. Bessa *et al.* (2021) performed an experimental study with respect to valve positioning, in the same aorta. A special configuration was designed to allow three-dimensional flow measurements at different cross-sections of the aorta. The velocimetry technique was implemented to generate instantaneous and average turbulent flow information for the variables of interest.

From the literature review, it is observed that the aortic valve is frequently modeled as a simple orifice. However, the influence of the leaflets is also discussed in the literature. Thus, in this study, the impact of a more realistic representation of the valve is investigated. The flow prediction obtained with a valve model representing the leaflets and a simplified representation of the valve as orifice, without the leaflets, is discussed. The analysis is performed, considering the most critical situation, corresponding the time instant of maximum flow rate during the systolic period, when the valve has its maximum opening.

2. METHODOLOGY

A computed tomography angiography (CTA) exam of a patient was selected for this analysis. This research was approved by the ethics committee of the National Institute of Cardiology, INC/MS. From a series of CTA slices, the DICOM (Digital Imaging and Communication in Medicine) images were transferred to the software Mimics (Materialise, Belgium) and an image segmentation was performed with the software FIJI (open-source image processing software based on ImageJ), generating a 3D model.

It is noteworthy that only the patient's aorta was obtained from the tomography, while the valve anatomy corresponding to its maximum opening was constructed using the SOLIDWORKS software, according to the valve images illustrated by Johnson *et al.* (2020). The orifice opening area was defined as 2 cm², equal to the area of the valve opening, based on measurements from electrocardiogram exam of the patient valve. The height of the leaflets was defined as 17 mm, based on the work of Matsushima *et al.* (2020), who presented information of the geometric height for tricuspid valves. Valve bulging was obtained according to ratios calculated by Kunihara (2017). Further information can be found in Gelio (2021).

To simulate the blood flow, the following hypotheses were defined. Gravity effects were neglected since the pressure variations are dominant over the force of gravity. The aorta surface was considered rigid, due to its small complacency (Ibanez *et al.*, 2020). Steady state flow was considered, by assuming that the pulsatile flow process can be represented as a succession of steady state flows (Celis *et al.*, 2020). Since body temperature is approximately constant (Hao, 2010), temperature variation was neglected. The blood was modeled as incompressible Newtonian fluid with constant viscosity μ=0.0035 Pa (Wang and Li, 2011), valid approximation for deformation rate superior to 50 s^{-1} (Crowley and Pizziconi, 2005). The density was set as ρ = 1054 kg/m^3 (Feijjo and Zouain, 1988). According to Gomes *et al.* (2017), the flow in the ascending aorta is turbulent, and the turbulence model κ-ω SST (Menter, 1994) was selected, as recommended by Celis *et al*. (2020).

Considering the hypotheses mentioned, the RANS conservation equations are

$$\frac{\partial u_j}{\partial x_j} = 0 \quad ; \quad \frac{\partial \rho u_j u_i}{\partial x_j} = -\frac{\partial \hat{p}}{\partial x_i} + \frac{\partial}{\partial x_j}\left[(\mu + \mu_t)\left(\frac{\partial u_i}{\partial x_j} + \frac{\partial u_j}{\partial x_i}\right)\right] \tag{1}$$

where u_j represents the time average velocity component, x_i are the coordinates axes, ρ is the blood density. $\hat{p}$ is a modified pressure, $\hat{p} = p + (2/3)\,\rho\,\kappa$, where κ is the turbulent kinetic energy. μ and μ_t are the molecular and turbulent viscosity, respectively. The turbulent viscosity of κ-ω SST turbulence model (Menter, 1994) is given by

$$\mu_t = \frac{\rho\,\kappa}{\omega}\xi_{\kappa-\omega} \tag{2}$$

where $\xi_{\kappa-\omega}$ is a blending factor between the $\kappa-\varepsilon$ and $\kappa-\omega$ models, and ω is the turbulent energy dissipation.

Figure 1 illustrates the aorta, with the three-dimensional valve model placed at the inlet, and different views of the aortic valve with a representation of the leaflets (Figure 1b). The human aorta has one inlet and four outlets: 1) brachiocephalic artery; 2) left common carotid artery; 3) left subclavian artery and 4) the main exit, which leads to the abdominal aorta (this region is called descending aorta (Alastruey *et al*., 2016). At the inlet, the maximum flow rate at the systole peak equal to 25 lt/min was defined. It was assumed a turbulence intensity of 5% (Celis *et al*., 2020). with a turbulent length scale equal to the inlet valve diameter. At the outlets, null diffusive flow condition was imposed in the normal exit direction for all variables, $\partial\,/\,\partial\,x_n = 0$. By following the works of Alastruey *et al. (*2016) the outflows mass flow rate distribution was defined based on average values in the human body, as a percentage of the inlet flow rate: 19.3% (brachiocephalic artery), 5.2% (left carotid artery), and 6.4% (left subclavian artery) and at the descending aorta the value was 69.1%.

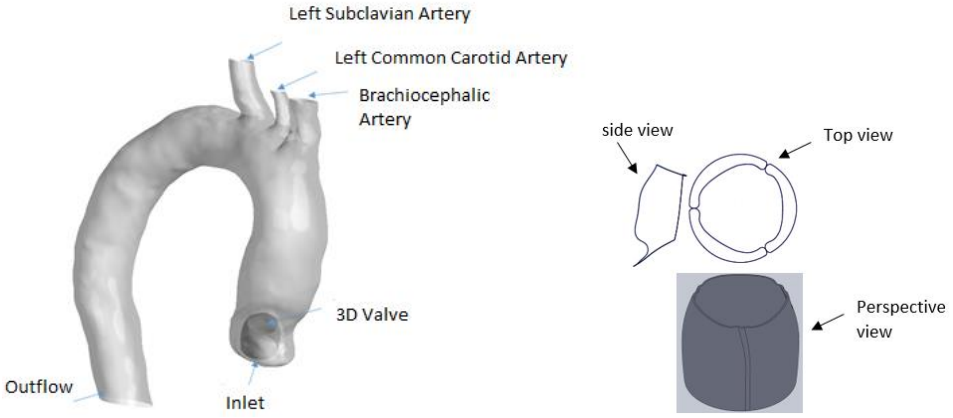

Figure 1. (a) Aorta representation, with a 3D valve, indication inlet and four outlets. (b) 3D valve model

The solution was obtained with the software Fluent 2020 (ANSYS Inc.), which is based on the finite volume method (Patankar, 1980). The results were post-processed with CFD-Post. The spatial discretization of the conservation equations was obtained with a second-order Upwind discretization scheme. For the coupling between pressure and velocity in the calculations, Fluent Coupled algorithm was used. The solution was considered converged when the residuals of all discretized equations reached values less than 10^{-6}. The computational mesh was generated using the same construction parameters for each case. The mesh definition was based on the mesh test performed by Ibanez *et al.* (2020) with 1.7 million elements. To check the adequacy of the mesh with the selected turbulence model, for both cases, it was verified that the value of $y^+ = \rho\,y\,u_\tau/\,\mu$ of the first nodal point along the entire aorta surface was below 5, where $u_\tau = (\tau_w/\,\rho)^{0.5}$ and $\tau_w$is the wall shear stress.

3. RESULTS AND DISCUSSION

To evaluate the impact on the aorta flow of the valve model in comparison with the valve orifice, it is presented in Figure 2, the streamlines colored with the turbulent kinetic energy. An acceleration of the flow through the valve, which has a convergence shape, can be observed. At the valve exit, the blood velocity is the same as at the orifice, since both have the same area, this at the valve height, the velocity for the orifice valve is smaller. Due to the valve height, the resulting inlet jet reaches a farther position at the aorta's interior. Near the aorta's arch, an equivalent complex flow structured is formed within both models, with strong recirculation. Also note that, the energy levels are quite similar, with slightly higher values due to the valve model, with the green and yellow-colored lines extending through the aortic arch, while for the aorta with the orifice, the lines with these colors end at the beginning of the aortic arch.

Another variable that can aid to analyze the flow, is an iso-surface of the Q-Criterion (Hunt *et al.* 1988) which helps to identify coherent flow structures. It is defined as

$$Q = \frac{1}{2}\left(\Omega_{ij}\Omega_{ij} - S_{ij}S_{ij}\right) \quad ; S_{ij} = \frac{1}{2}\left[\frac{\partial\,u_i}{\partial\,x_j} + \frac{\partial\,u_j}{\partial\,x_j}\right] \quad ; \quad \Omega_{ij} = \frac{1}{2}\left[\frac{\partial\,u_i}{\partial\,x_j} - \frac{\partial\,u_j}{\partial\,x_j}\right] \tag{3}$$

where S_{ij} is the strain rate tensor of the fluid element and Ω_{ij} is the vorticity tensor. A positive Q value means that the magnitude of the vortex outweighs the strain rate. Biasetti *et al.* (2011) correlated vertical structures with high levels of shear stress in aortas with abdominal aneurysms. Thus, the identification of these structures within the ascending aorta is also relevant, and the impact of the valve model on coherent structures formation is shown in Figure 3.

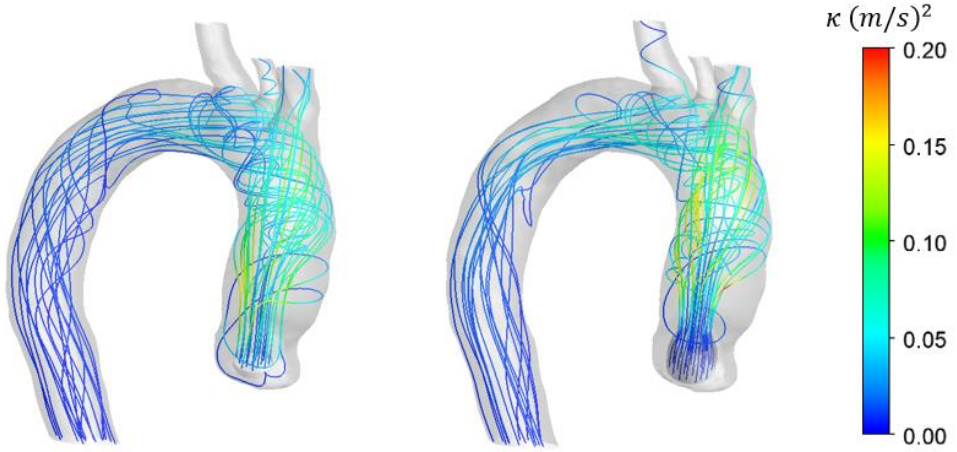

(a) valve as a circular orifice (b) three-dimensional (3D) valve

Figure 2. Streamlines with contours of turbulent kinetic energy

Alongside with the Q-criterion, another important quantity will be used, the normalized helicity

$$H = \xi_i \frac{u_i}{\left[\sqrt{\xi_k\,\xi_k}\;\sqrt{u_\ell\,u_\ell}\right]} \;\; ; \quad \xi_i = \epsilon_{ijk}\frac{\partial\, u_j}{\partial x_i} \tag{4}$$

where ξ_i is the vorticity and ϵ_{ijk} the Levi-Civita operator. The helicity evaluates the tendency of the flow to form vortices, representing the amount of connection of the vortex lines of the flow. The helical flow can promote aortic dilation. Therefore, the normalized helicity can help in the characterization of valvar and heart diseases. Helicity values of 1 or −1 represent the vortex core, which is characterized by strong vortex winding. Several researchers (e.g.: Gallo et al (2012) indicate that an absolute normalized helicity value greater than 0.6 represents the possibility of vascular remodeling.

Figure 3 shows iso-surfaces of Q, colored with normalized helicity for both valve models. It is conceivable to detect, qualitatively for both cases, very similar iso-surfaces, and similar helicity contours. Almeida *et al.* (2021) identified a similar flow structure, comparable to a hairpin shape for a group of patients and mentioned that it might have a correlation with aortic aneurysms growth. A comparison of the two cases, shows in the aorta with the orifice, the hairpin structure is better defined and has higher helicity values on the iso-surface of Q. The presence of the valve model created a toroidal structure at its exit, but the flow structure at most of the ascending aorta is very similar.

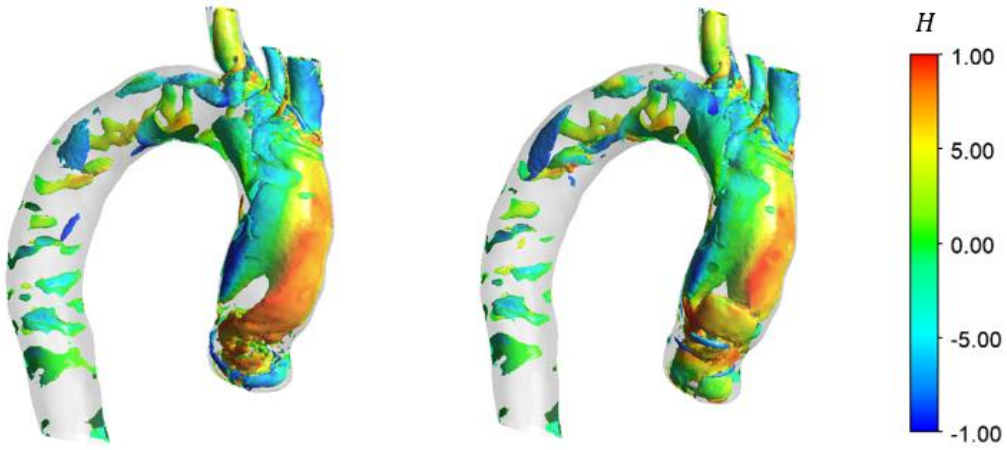

(a) valve as a circular orifice (b) three-dimensional (3D) valve

Figure 3. Q-Criterion with normalized helicity

Pressure and wall shear stress (WSS) distributions on the walls of the aorta are crucially to the health of a human being and these can be related to the growth of aneurysms in the ascending aorta (Almeida *et al.*, 2021). Therefore, a comparison of the prediction obtained with and without the valve model for these two quantities are examined in Figure 4 and Figure 5.

Figure 4 reveals the pressure distribution on the surface of the aorta for both cases. It is important to highlight the similarities between the pressure levels, as well as the jet impact region on the wall. This confirms, once again, the hypothesis that approximation of the valve as a circular orifice is feasible for this variable. Furthermore, it is possible to

detect slightly higher-pressure levels in the jet incidence region, which is a consequence of the higher jet value at the physical valve exit, as shown above. It is also noted that in the aortic root, pressure levels are higher for the case with the circular orifice. This is also because the flow is accelerated until it reaches the exit of the physical valve, with low intensity recirculation between the valve and the surface of the aorta in this region.

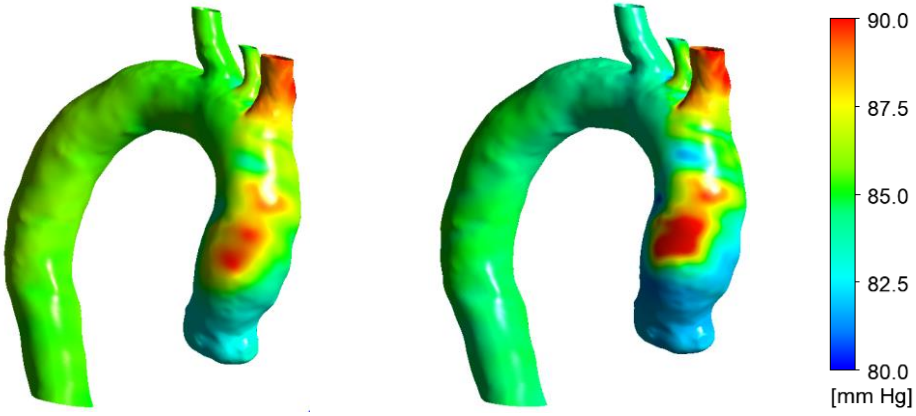

(a) valve as a circular orifice (b) three-dimensional (3D) valve

Figure 4. Pressure levels of the aorta with a circular opening and with valve during maximum flow

Figure 5 illustrates the WSS on the surface of the aorta. As mentioned, the effect of WSS on the aortic wall is a parameter closely connected with aortic dilation and aortic aneurysms. Its highest values are in the region of the ascending aorta, where the jet impinges the aortic wall, where pressure is also high. For both cases, the WSS fields are similar however, the aorta with the 3D valve has a larger region with high shear stress values, as the presence of the valve leads to higher jet velocities, and consequently higher shear stresses, when compared with the case with the valve as an orifice. Additionally, it was observed lower shear stress levels in the aortic root, which can be related to low velocity recirculation around the valve.

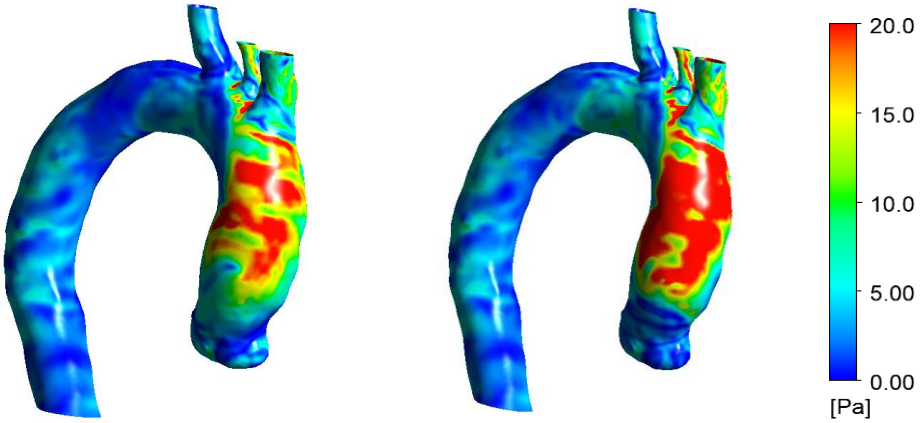

(a) valve as a circular orifice (b) three-dimensional (3D) valve

Figure 5. Wall shear stress distribution the aorta with a circular opening and with valve during maximum flow

Table 1 presents the mean and maximum values of pressure and shear stress at the region of interest, where the jet impacts in the ascending aorta. The pressures obtained for the two cases are very similar. It is observed that the physical valve leads to slightly higher values of maximum pressure on the surface of the aorta, while the mean pressure is slightly lower. However, the maximum WSS is much higher in the case of the physical valve, reinforcing the previous analysis.

Table 1. Average and maximum pressure and shear stress values in the region of interest.

Quantity	**Circular orifice**	**3D valve**
Maximum pressure at the interest region [mmHg]	90.0	91.8
Average pressure at the interest region [mmHg]	84.8	83.4
Maximum WSS at the interest region [Pa]	33.2	51.8
Average WSS at the interest region [Pa]	7.6	9.6

4. CONCLUSIONS

In the present study, it was investigated the impact of the anatomy of the aortic valve model on the behavior of blood flow in the ascending aorta and aortic arch during the systole peak, corresponding to the maximum flow rate, when the aortic valve is fully opened. To this end, the flow prediction was compared with the results obtained considering the valve as a simple circular orifice.

The flow pattern obtained with both valve configurations is very similar. In the region of the aortic root, the velocities are increasing in the case of the valve model representing the leaflets, also, at this region the velocity in the case of valve orifice is decreasing because loses momentum as it flows. Further, a toroidal structure is formed as the flow leaves the valve model. Moreover, near the aortic root, between the valve and aortic wall, recirculation was observed, associated with lower pressure levels. Slightly higher turbulent quantities are present for the valve model at the region of the jet impact on the aorta.

Both models presented similar wall pressure and shear stress distributions, with equivalent blood jet impact region on the wall of the ascending aorta. However, due to the higher velocity at the leaflets height of the valve model, slightly larger region with high pressure and higher WSS were obtained at the aortic wall, for the valve model representing the leaflets case.

From all the hemodynamic results obtained, it is possible to conclude that the use of the circular orifice in place of the valve model representing the leaflets is an acceptable strategy when one wants to make a first assessment regarding the map of normal and tangential tensions in the wall of the ascending aorta and aortic arch.

5. ACKNOWLEDGEMENTS

This work was supported by the Cardiovascular Engineering Laboratory PUC-Rio. The authors also thank the Brazilian government agencies CNPq and CAPES for the continuous support.

6. REFERENCES

Alastruey, J., Xiao, N., Fok, H., Schaeffter, T., and Figueroa, C. A., 2016. “On the impact of modelling assumptions in multi-scale, subject-specific models of aortic haemodynamics”. *Journal of the Royal Society Interface*, Vol. 13, No. 119, pp. 1-17

Almeida, G. C., Azevedo, B. A., Azevedo, F. S., Kalaoun, K., Ibanez, I., Teixeira, P. S., Gottieb, I., Nelo, M.M., Oliveira, G.M.M. and Nieckele, A. O., 2021. “Computational Fluid Dynamics to Access the Future Risk of Ascending Aortic Aneurysms”. *Arquivos Brasileiros de Cardiologia, in press.*

Becsek, B., Pietrasanta, L., and Obrist, D. 2020., “Turbulent systolic flow downstream of a bioprosthetic aortic valve: velocity spectra, wall shear stresses, and turbulent dissipation rates*”. Frontiers in Physiology*, Vol. 11, pp. 1169.

Bessa, G. M., Fernandes, L. S., Gomes, B. A., and Azevedo, L. F., 2021. “Influence of aortic valve tilt angle on flow patterns in the ascending aorta”. *Experiments in Fluids*, Vol. 62, No. 5, pp.1-31.

Biasetti, J., Hussain, F., and Gasser, T. C., 2011., “Blood flow and coherent vortices in the normal and aneurysmatic aortas: a fluid dynamical approach to intra-luminal thrombus formation”. *Journal of the Royal Society Interface*, Vol. 8, No. 63, pp. 1449-1461.

Celis, D., Gomes, B. A. d. A., Ibanez, I., Azevedo, P. N., Teixeira, P. S., and Nieckele, A. O. 2020. “Prediction of Stress Map in Ascending Aorta-Optimization of the Coaxial Position in Transcatheter Aortic Valve Replacement”. *Arquivos Brasileiros de Cardiologia*, Vol. 115, No. 4, pp. 680-687.

Crowley, T. A., and Pizziconi, V. 2005. “Isolation of plasma from whole blood using planar microfilters for lab-on-a-chip applications”. *Lab on a Chip*, Vol. 5, No. 9, pp. 922-929.

Feijóo, R., and Zouain, N. 1988. “Formulations in rates and increments for elastic-plastic analysis”. *International Journal for Numerical Methods in Engineering*, Vol. 26, No. 9, pp. 2031-2048.

Fries, R., Graeter, T., Aicher, D., Reul, H., Schmitz, C., Böhm, M., and Schäfers, H.-J. 2006. “In vitro comparison of aortic valve movement after valve-preserving aortic replacement”. *The Journal of Thoracic and Cardiovascular Surgery*, Vol. 132, No.1, pp. 32-37.

Gallo D, Steinman DA, Bijari PB, and Morbiducci U. 2012 “Helical flow in carotid bifurcation as surrogate marker of exposure to disturbed shear”. *Journal of Biomechanics*. Vol. 45, No. 14, pp. 2398-2404

Gelio, R.M.L. 2021. *Influence of simplified models of aortic valves in the ascending aorta blood flow* (in Portuguese). Final Undergraduate Project, Mechanical Engineering, PUC-Rio, Rio de Janeiro, RJ, Brazil.

Gomes, B. A. d. A., Camargo, G. C., Santos, J. R. L. d., Azevedo, L. F. A., Nieckele, A. O., Siqueira-Filho, A. G., and Oliveira, G. M. M. d. 2017. “Influence of the tilt angle of percutaneous aortic prosthesis on velocity and shear stress fields”. *Arquivos Brasileiros de Cardiologia*, Vol. 109, No. 3, pp. 231-240.

Haj-Ali, R., Marom, G., Zekry, S. B., Rosenfeld, M., and Raanani, E. 2012. "A general three-dimensional parametric geometry of the native aortic valve and root for biomechanical modeling". *Journal of Biomechanics*, Vol. 45, No.14, pp. 2392-2397.

Hao, Q. 2010. *Modeling of Flow in an In Vitro Aneurysm Model. A Fluid-Structure Interaction Approach*. Doctoral Dissertation, University of Miami, Miami, Fl, USA.

Hunt, J. C., Wray, A. A., and Moin, P. 1988. "Eddies, streams, and convergence zones in turbulent flows". *Proceedings of the 1988 Summer Program*, Center of Turbulence Research, pp. 193-208.

Ibanez, I., de Azevedo Gomes, B. A., and Nieckele, A. O. 2020. "Effect of percutaneous aortic valve position on stress map in ascending aorta: A fluid-structure interaction analysis". *Artificial Organs*. doi: 10.1111/aor.13883.

Johnson, E. L., Wu, M. C., Xu, F., Wiese, N. M., Rajanna, M. R., Herrema, A. J., and Hsu, M.-C. 2020. "Thinner biological tissues induce leaflet flutter in aortic heart valve replacements". *Proceedings of the National Academy of Sciences*, Vol. 117, No. 32, pp. 19007-19016.

Katsi, V., Magkas, N., Antonopoulos, A., Trantalis, G., Konstantinos, T., and Tousoulis, D. 2020. "Aortic Valve: Anatomy and Structure and the Role of Vasculature in the Degenerative Process". *Acta Cardiologica*. pp. 1–14

Kunihara, T. 2017. "Anatomy of the aortic root: implications for aortic root reconstruction". *General thoracic and cardiovascular surgery*, Vol. 65, pp. 488-499.

Leyh, R. G., Schmidtke, C., Sievers, H.-H., and Yacoub, M. H. 1999. "Opening and closing characteristics of the aortic valve after different types of valve-preserving surgery". *Circulation*, Vol. 100, No. 21, pp. 2153-2160.

Matsushima, S., Karliova, I., Gauer, S., Miyahara, S., and Schäfers, H. J. 2020. "Geometry of cusp and root determines aortic valve function". Indian Journal of Thoracic and Cardiovascular Surgery, Vol. 36, No. 1, pp. 64-70.

Menter, F. R. 1994. "Two-equation eddy-viscosity turbulence models for engineering applications". *AIAA journal*, Vol. 32, No. 8, pp. 1598-1605.

Patankar, S. 1980. "Numerical heat transfer and fluid flow": *CRC press*.

Piazza, N., de Jaegere, P., Schultz, C., Becker, A. E., Serruys, P. W., and Anderson, R. H. 2008. "Anatomy of the aortic valvar complex and its implications for transcatheter implantation of the aortic valve". *Circulation: Cardiovascular Interventions*, Vol. 1, No. 1, pp. 74-81.

Sahasakul, Y., Edwards, D. W., Naessens, M. J., and Tajik, J. A. 1988. "Age-Related Changes in Aortic and Mitral Valve Thickness: Implications for Two-Dimensional Echocardiography Based on an Autopsy Study of 200 Normal Human Hearts." *The American Journal of Cardiology* Vol. 62, No. 7: pp. 424-430.

Simão, M., Ferreira, J., Tomás, A. C., Fragata, J., and Ramos, H. 2017. "Aorta ascending aneurysm analysis using CFD models towards possible anomalies". *Fluids*, Vol. 2, No. 2, pp. 31.

Tang, A., Fan, Y., Cheng, S., and Chow, K. 2012. "Biomechanical factors influencing type B thoracic aortic dissection: computational fluid dynamics study." *Engineering Applications of Computational Fluid Mechanics*, Vol. 6, No. 4, pp. 622-632.

Wang, X., and Li, X. 2011. "Biomechanical behaviors of curved artery with flexible wall: A numerical study using fluid–structure interaction method". *Computers in Biology and Medicine*, Vol. 41, No. 11, pp. 1014-1021.

Yuan, S.M., and Jing, H., 2010. "The bicuspid aortic valve and related disorders". *Sao Paulo Medical Journal*, Vol. 128, No. 5, pp. 296-301.

7. RESPONSIBILITY NOTICE

The authors are the only responsible for the printed material included in this paper.